




## FULL PAPER

# The effects of morin and methotrexate on pentose phosphate pathway enzymes and GR/GST/TrxR enzyme activities: An in vivo and in silico study

Cuneyt Caglayan<sup>1</sup>  | Yusuf Temel<sup>2</sup> | Cüneyt Türkeş<sup>3</sup> | Adnan Ayna<sup>4</sup> |  
Abdulilah Ece<sup>5</sup>  | Şükrü Beydemir<sup>6,7</sup> 

<sup>1</sup>Department of Medical Biochemistry, Faculty of Medicine, Bilecik Şeyh Edebalı University, Bilecik, Turkey

<sup>2</sup>Department of Solhan School of Health Services, Bingöl University, Bingöl, Turkey

<sup>3</sup>Department of Biochemistry, Faculty of Pharmacy, Erzincan Binalı Yıldırım University, Erzincan, Turkey

<sup>4</sup>Department of Chemistry, Faculty of Sciences and Arts, Bingöl University, Bingöl, Turkey

<sup>5</sup>Department of Pharmaceutical Chemistry, Faculty of Pharmacy, Biruni University, İstanbul, Turkey

<sup>6</sup>Department of Biochemistry, Faculty of Pharmacy, Anadolu University, Eskişehir, Turkey

<sup>7</sup>Bilecik Şeyh Edebalı University, Bilecik, Turkey

## Correspondence

Cuneyt Caglayan, Department of Medical Biochemistry, Faculty of Medicine, Bilecik Şeyh Edebalı University, Bilecik 11230, Turkey.

Email: [cuneyt.caglayan@bilecik.edu.tr](mailto:cuneyt.caglayan@bilecik.edu.tr)

## Funding information

This work was supported by Grants from the Scientific Research Projects Coordination Unit of Bingöl University.

## Abstract

In this study, the mechanisms by which the enzymes glucose-6-phosphate dehydrogenase (G6PD), 6-phosphogluconate dehydrogenase (6PGD), glutathione reductase (GR), glutathione-S-transferase (GST), and thioredoxin reductase (TrxR) are inhibited by methotrexate (MTX) were investigated, as well as whether the antioxidant morin can mitigate or prevent these adverse effects in vivo and in silico. For 10 days, rats received oral doses of morin (50 and 100 mg/kg body weight). On the fifth day, a single intraperitoneal injection of MTX (20 mg/kg body weight) was administered to generate toxicity. Decreased activities of G6PD, 6PGD, GR, GST, and TrxR were associated with MTX-related toxicity while morin treatment increased the activity of the enzymes. The docking analysis indicated that H-bonds, pi-pi stacking, and pi-cation interactions were the dominant interactions in these enzyme-binding pockets. Furthermore, the docked poses of morin and MTX against GST were subjected to molecular dynamic simulations for 200 ns, to assess the stability of both complexes and also to predict key amino acid residues in the binding pockets throughout the simulation. The results of this study suggest that morin may be a viable means of alleviating the enzyme activities of important regulatory enzymes against MTX-induced toxicity.

## KEYWORDS

antioxidant system, methotrexate, molecular dynamics, morin, thioredoxin reductase

**Abbreviations:** 3PG, 3-phosphoglyceric acid; 6PGD, 6-phosphogluconate dehydrogenase; BSA, bovine serum albumin; CBL, chlorambucil; CDNB, 1-chloro-2,4-dinitrobenzene; DTNB, 5,5'-dithiobis(2-nitrobenzoic acid); G6PD, glucose-6-phosphate dehydrogenase; GR, glutathione reductase; GSSG, glutathione disulfide; GST, glutathione-S-transferase; HXP, 3,6-dihydroxy-xanthene-9-propionic acid; KCl, potassium chloride; LSD, least significant difference; MD, molecular dynamic; MM-GBSA, molecular mechanics with generalized Born and surface area solvation; MTX, methotrexate; NADP<sup>+</sup>, nicotinamide adenine dinucleotide phosphate; NADPH, reduced nicotinamide adenine dinucleotide phosphate; OPLS, optimal potential liquid simulations; PDB, Protein Data Bank; RA, rheumatoid arthritis; RMSD, root mean square deviation; RMSF, root mean square fluctuations; TPT, 2,2':6',2''-terpyridine platinum(II) chloride; TrxR, thioredoxin reductase; XP, extra precision.

## 1 | INTRODUCTION

Rheumatoid arthritis (RA) is a chronic autoimmune inflammatory illness that has a negative impact on one's quality of life and severely affects bones and joints.<sup>[1]</sup> As a folate analog and selective antagonist to folic acid enzymes, methotrexate (MTX) is used to treat various autoimmune disorders, dermatological conditions, and cancers, and also to end pregnancies.<sup>[2]</sup> Low dosages of MTX (0.4 mg/kg/week) reduce inflammation in RA patients via altering adenosine signaling, but high doses of MTX prevent cancer cells from synthesizing folic acid. Due to MTX's antifolate characteristics, continuous use of the drug even at modest dosages can result in a variety of side effects, including gastrointestinal ulcers, myelosuppression, and liver and renal failure.<sup>[3]</sup> One strategy to ameliorate the negative effects of MTX in therapeutic applications might be to protect the organs from unfavorable side effects. Because of this, natural biomolecules with antioxidant properties that may lessen the severity of MTX-induced toxicities may be helpful for therapeutic purposes.

One of the main ingredients of many food crops and medicinal plants that are suggested in conventional medicine for the treatment of many human diseases is morin, a dietary flavanol. Several fruits and vegetables including fig, mulberry, onion, and apple contain morin.<sup>[4,5]</sup> Two benzene rings joined by a heterocycle pyrone ring make up the chemical structure of morin (3,5,7,2',4'-pentahydroxyflavone), which also has five hydroxy substituents at positions 2', 4', 3, 5, and 7.<sup>[6]</sup> Due to its intriguing medicinal potential, this dietary flavanol has received a lot of interest over the last 10 years. Numerous *in vivo* and *in vitro* research have revealed the pleiotropic effects of morin. Researchers have discovered that morin covers antioxidant, anti-inflammatory, neuroprotective, anti-hyperlipidemic, antihypertensive, antidiabetic, antibacterial, antiallergic, and anticancer properties.<sup>[4,7-9]</sup> According to studies, morin significantly reduces the toxicity and side effects of a number of drugs without impairing their intended functions.

No study has been found examining the effects of MTX on pentose phosphate pathway regulatory enzymes, glutathione antioxidant system and thioredoxin antioxidant system, which are important for metabolism. This study sought to understand how MTX inhibits glucose-6-phosphate dehydrogenase (G6PD, EC.1.1.1.49), 6-phosphogluconate dehydrogenase (6PGD, EC.1.1.1.44), glutathione reductase (GR, EC.1.6.4.2), glutathione-S-transferase (GST, EC.2.5.1.18), and thioredoxin reductase (TrxR, EC.1.6.4.5) enzymes as well as if morin, a natural antioxidant, can prevent or lessen these negative effects *in vivo*.

## 2 | RESULTS AND DISCUSSION

### 2.1 | Effects of methotrexate and morin on enzyme activities

*In vivo* effect of morin (100 mg/kg), MTX (20 mg/kg), and MTX +morin (50 and 100 mg/kg) on rat erythrocyte pentose pathway enzymes (G6PD and 6PGD) enzyme activities were studied. The results indicated that MTX treatment significantly reduced the

activities of both enzymes while treatment of MTX+morin restored the activities of both enzymes (Figure 1c,d).

When *in vivo* effects of morin (100 mg/kg), MTX (20 mg/kg), and MTX+morin (50 and 100 mg/kg) on GR enzyme activity were evaluated it was found that GR enzyme activity meaningfully decreased in the MTX-treated group. The treatment of MTX with different doses of morin (50 and 100 mg/kg) increased the activity of the enzyme for which a 50 mg/kg dose of morin showed better ameliorative effects (Figure 2a). Morin and MTX+morin (50 mg/kg) treatment significantly increased the activity of GR in comparison to the untreated control group.

The *in vivo* effect of MTX and ameliorative effects of morin treatment at 50 and 100 mg/kg doses were investigated on the activity of GST. It was revealed that the enzyme activity of GST was significantly reduced in the MTX-treated group. The treatment of MTX with different doses of morin (50 and 100 mg/kg) alleviated the activity of the enzyme in similar manners (Figure 2b). Morin treatment alone significantly increased the activity of GST in comparison to the untreated control group.

We also investigated the *in vivo* effects of morin (100 mg/kg), MTX (20 mg/kg), and MTX+morin (50 and 100 mg/kg) on TrxR enzyme activity. Our results demonstrated that the enzyme activity of TrxR was significantly reduced in the MTX-treated group. Treatment of MTX with different doses of morin (50 and 100 mg/kg) apparently did not alleviate the toxic effects of MTX on TrxR enzyme activity (Figure 2c). Morin treatment alone did not alter the activity of TrxR as compared with the untreated control group.

MTX is used to treat inflammatory and autoimmune illnesses. It is a folic acid antagonist commonly used to treat breast cancer, leukemia, and osteosarcoma.<sup>[10]</sup> The enzyme dihydrofolate reductase, which catalyzes the interconversion of dihydrofolate to tetrahydrofolate, which is necessary for nucleotide synthesis, is inhibited by MTX. Additionally, MTX was found to limit *de novo* purine production. Because of this, MTX prevents the production of DNA, RNA, and protein, which ultimately results in death in the cells or tissues.<sup>[11,12]</sup> However, MTX has toxicity not only against malignant cells but also for healthy organs like the liver,<sup>[13]</sup> kidney,<sup>[14]</sup> testes,<sup>[15]</sup> and brain.<sup>[16]</sup> As a result, alleviating MTX's toxicity and understanding its adverse effects might lead to better treatment, higher adherence, and lower mortality. To the extent of our knowledge, there is no study focusing on the possible effects of MTX and morin on the activities of some crucial metabolic enzymes such as G6PD, 6PGD, GR, GST, and TrxR in rats. Therefore, the aim of the current research was to determine the curative effects of morin on MTX-induced enzyme inhibitions.

Research on drug-enzyme interactions and metabolic enzymes is becoming more and more noteworthy in recent decades. Due to its possible involvement in a number of disorders, GST has been the focus of numerous types of research. It has various biological functions. It is consistently strongly expressed in a variety of cancer cell types, including osteosarcoma, melanoma, lymphoma, and human breast, colon, liver, pancreas, stomach, and uterine malignancies.<sup>[17]</sup> A compound that inhibits GST can have potent anticancer effects on cancer cells while ameliorating toxicity for healthy cells. There has been a lot of research about the effects of various pharmaceuticals

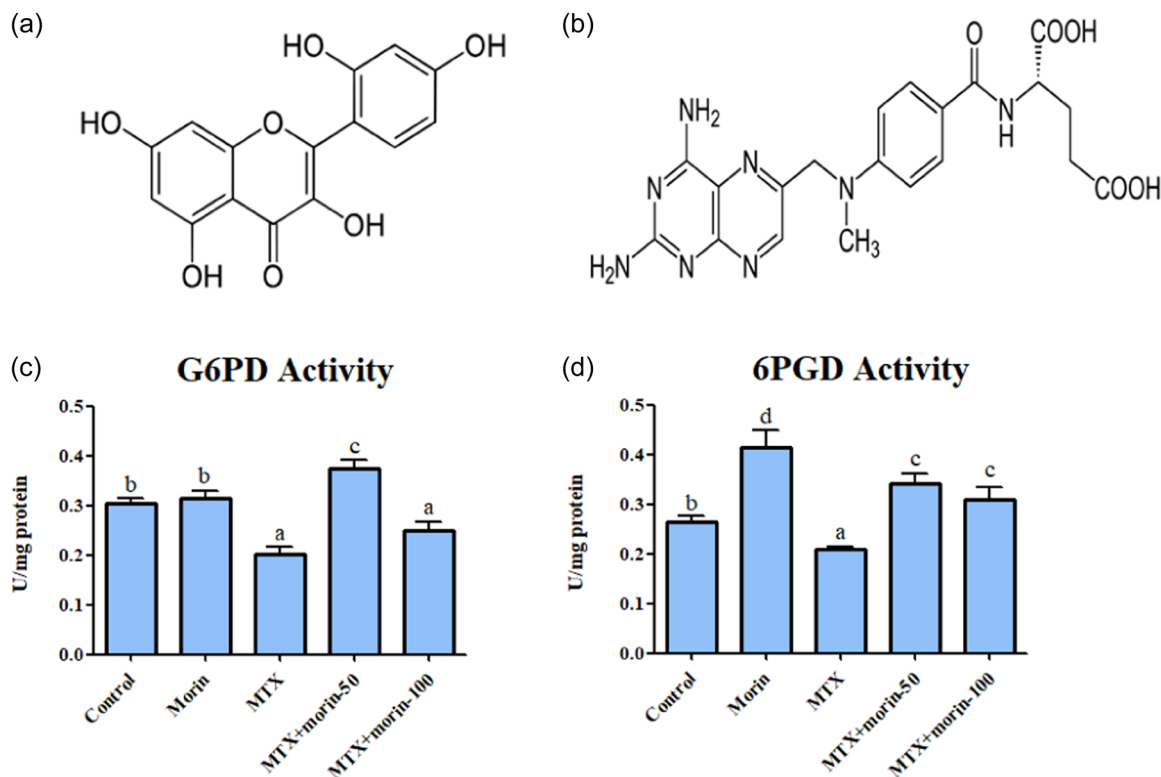


**FIGURE 1** (a) Chemical structure of morin. (b) Chemical structure of methotrexate. (c) The inhibitory effect of methotrexate and morin on glucose-6-phosphate dehydrogenase (G6PD) enzyme activity. (d) The inhibitory effect of methotrexate and morin on 6-phosphogluconate dehydrogenase (6PGD) enzyme activity. Different letters (a–d) indicate statistical differences among the groups ( $p < 0.05$ ).

and organic compounds on GSTs, but none have examined the inhibitory activity and mechanism of morin and MTX on GST. Therefore, in this investigation, we focussed on the *in vivo* inhibition of GST enzyme activity by MTX and the role of morin in reducing this effect. Our results revealed that the enzyme activity of GST was significantly reduced in the MTX-exposed group. Treatment of MTX with different doses of morin (50 and 100 mg/kg) increased the activity of the enzyme in similar manners. Cefazolin, cefuroxime, and cefaperazon were studied for their ability to inhibit GST in albino-rat heart, liver, and kidney tissues by Türkan et al.<sup>[18]</sup> They discovered that cefazolin had no inhibitory effects on GST in any of the worked tissues, and that cefazolin and cefuroxime reduced GSST activity after the fifth hour. In a different study, Türkan et al. also used *in vitro* and molecular docking procedures to examine the inhibitory effects of carbamazepine, chlorpromazines, isoprenaline, and tamoxifen on GST.<sup>[19]</sup> They stated that all of the drugs they examined effectively inhibited the GST enzyme, and that chlorpromazine was the best inhibitor, with a  $K_i$  value of  $42.83 \pm 8.52$  nM. Gentamicin and clindamycin both inhibited the enzymatic activity of human erythrocyte GST, with  $IC_{50}$  values of 1.69 and 6.9 mM and  $K_i$  constants of 1.70 and 2.36 mM, respectively, as reported by Ayna et al.<sup>[20]</sup> They also found that the activity of the GST was stimulated by scopolamine butylbromide and ampicillin, but not by cefazolin.

G6PD is an enzyme that plays a fundamental role in cellular metabolism, particularly in the pentose phosphate pathway. It catalyzes the conversion of G6P to 6-phosphogluconolactone, while

simultaneously reducing nicotinamide adenine dinucleotide phosphate (NADP<sup>+</sup>) to its reduced form, NADPH. It is primarily found in the liver, but it is also present in other tissues, such as red blood cells. This pathway is important for the production of NADPH, which is necessary for many cellular processes, including the synthesis of fatty acids and cholesterol and the detoxification of reactive oxygen species.<sup>[21]</sup> G6PD deficiency is an inherited genetic disorder that affects the activity or production of the G6PD enzyme. This primarily affects red blood cells and is more common in males. G6PD deficiency can result in hemolytic anemia, a condition where red blood cells are more susceptible to damage and premature destruction, especially when exposed to certain triggers such as infections, certain medications, or consumption of certain foods. This can cause symptoms such as fatigue, jaundice, and dark urine.<sup>[22]</sup> Researchers have isolated the G6PD and 6PGD enzymes from different tissues and examined how chemicals and treatments affect their ability to function. In a study, Temel et al.<sup>[23]</sup> isolated the G6PD enzyme from rat erythrocytes with a specific activity of 29.20 EU/mg proteins. Then they discovered how rat erythrocyte G6PD enzyme activity was affected by several antibiotics. The enzyme activity of G6PD was suppressed by furosemide, gentamicin, and clindamycin with  $K_i$ s of 0.86, 0.70, and 39.80 mM, respectively. G6PD and 6PGD enzymes from rat hearts were isolated by Adem and Ciftci<sup>[24]</sup> who also investigated the inhibitory effects of dopamine, furosemide, and digoxin on these enzyme activities. The inhibitory effect of these agents was low. Kizilbay and Karaman<sup>[25]</sup> purified G6PD at a

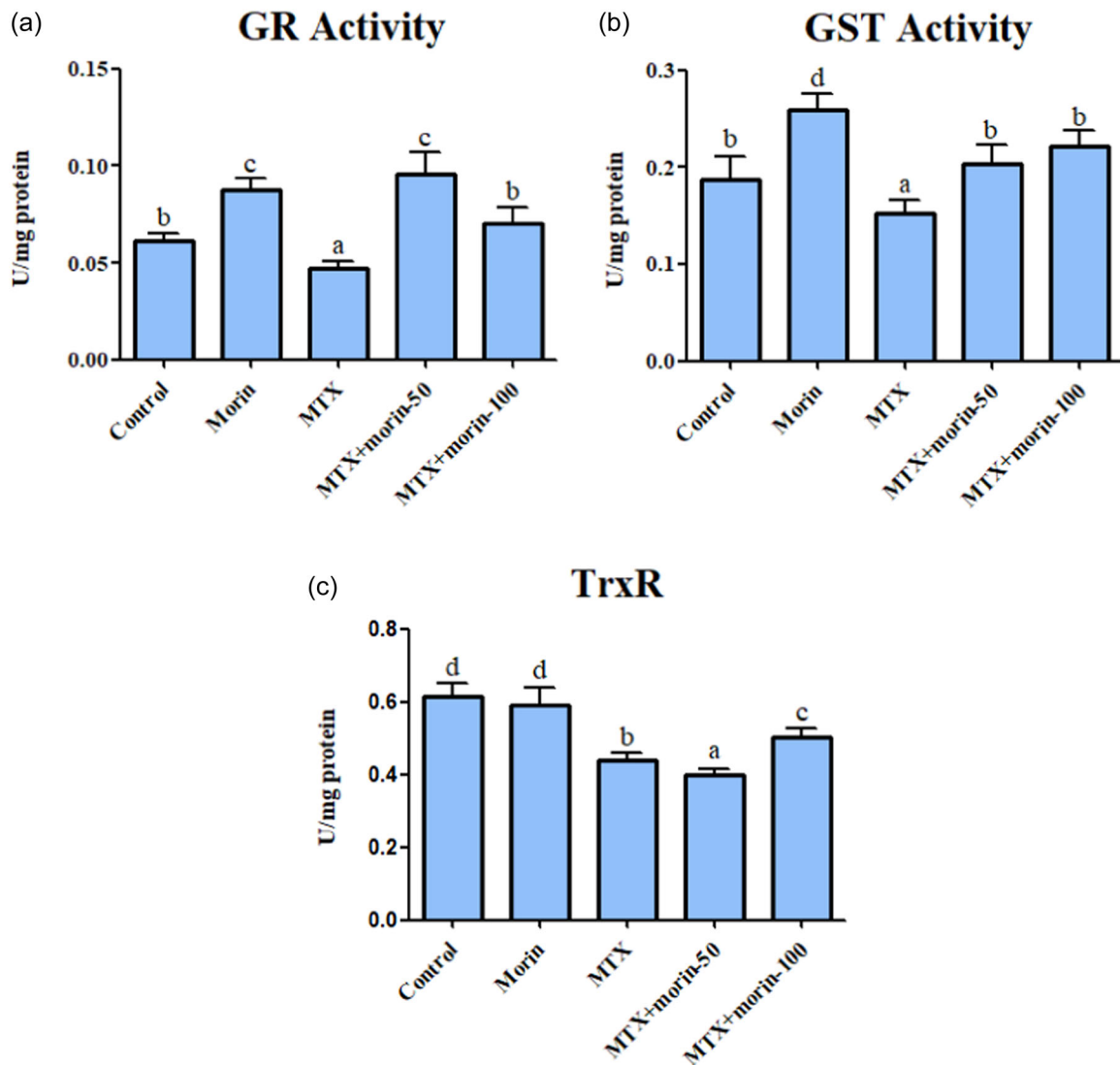


**FIGURE 2** (a) The inhibitory effect of methotrexate and morin on glutathione reductase (GR) enzyme activity. (b) The inhibitory effect of methotrexate and morin on glutathione-S-transferase (GST) enzyme activity. (c) The inhibitory effect of methotrexate and morin on thioredoxin reductase (TrxR) enzyme activity. Different letters (a–d) indicate statistical differences among the groups ( $p < 0.05$ ).

219.81-fold efficiency and ascertained dobutamine hydrochloride's *in vivo* inhibitory effects. Effects of several drugs including MTX were tested for their effects on G6PD by Akkemik et al.<sup>[26]</sup> The range of  $K_i$  constants was  $0.0052 \pm 0.0012$  to  $48.4380 \pm 2.176$  mM. Çalışkan et al.<sup>[27]</sup> isolated GR, G6PD, and  $\delta$ PGD from human erythrocytes and identified the inhibitory profile of these enzymes for proparacaine and brimonidine.  $K_i$  values for proparacaine and brimonidine for  $\delta$ PGD were  $811.50 \pm 11.13$  and  $66.06 \pm 0.78$   $\mu$ M, respectively.

GR is an enzyme that plays a vital role in the cellular antioxidant defense system. It is responsible for maintaining the reduced state of GSH, a critical molecule involved in protecting cells from oxidative stress.<sup>[28]</sup> GR catalyzes the reduction of glutathione disulfide (GSSG) using NADPH. The stability of the GSH/GSSG ratio in the cell environment is the main objective of the GR enzyme-catalyzed process. In addition to preserving the GSH/GSSG ratio, it also aids in the continuation of crucial cellular functions such as ROS detoxification.<sup>[29]</sup>

According to the previous studies regarding GR, the fluorophenylthiourea compounds displayed low  $\mu$ M  $IC_{50}$  and  $K_i$  values, with  $IC_{50}$  values ranging from  $8.85 \pm 0.20$  to  $21.62 \pm 0.27$   $\mu$ M and  $K_i$  constants from  $23.04 \pm 4.37$  to  $59.97 \pm 13.45$   $\mu$ M.<sup>[30]</sup> Li et al.<sup>[31]</sup> investigated the time- and concentration-dependent inhibition of yeast GR and human GR by phenethyl and benzyl isothiocyanates. The inhibiting effects of *N*-methylpyrrole derivatives on GR were described by Kocaoğlu et al.<sup>[32]</sup> All the agents tested outperformed the potent GR inhibitor *N,N*-bis(2-chloroethyl)-*N*-nitrosourea in terms of inhibitory efficacy, which researchers discovered. An investigation on how different antioxidant compounds (curcumin, quercetin, and resveratrol) affect the activity of GR revealed that curcumin, quercetin, and resveratrol each had  $IC_{50}$  values of 17.25, 57.8, and 520  $\mu$ M, respectively.<sup>[33]</sup>

A unique strategy to combat various diseases is to target TrxR by administering TrxR inhibitors. According to Tiwari et al.<sup>[34]</sup> 1-chloro-2,4-dinitrobenzene (CDNB) impairs the survival of filarial

parasites by permanently blocking the cysteine in the enzyme's active site. Synthetic curcumin analog B5 inhibits TrxR and causes induction of apoptosis in the cervical cancer cell lines.<sup>[35]</sup> TrxR inhibitors can bind to the enzyme's two redox sites, the NADPH binding site, the Cys residues in those sites, or other locations. Upon reduction by NADPH, the highly reactive and nucleophilic Cys residue is exposed on the surface of the enzyme as a result of this reduction. TrxR1's capability to decrease Trx and selenite is prevented by inhibitors that bind the enzyme's Cys. Some TrxR inhibitors are known suicide substrates, which alkylate or otherwise covalently modify reactive Cys residues of the two main redox sites of the enzyme.<sup>[36]</sup>

## 2.2 | In silico study

Molecular docking calculations can contribute a thorough insight into the compound's mode of action including whether it operates as an agonist or antagonist. Here, assuming compounds have competitive inhibition, to examine the behavior of MTX and morin in the binding regions of the 6PGD, G6PD, GR, GST, and TrxR enzymes, a thorough SAR research was conducted. The performance of the Glide XP docking protocol was evaluated by re-docking the cocrystallized native ligands, 3PG (3-phosphoglyceric acid), NAP (NADP), HXP (3,6-dihydroxy-xanthene-9-propionic acid), CBL (chlorambucil), and TPT (2,2':6',2''-terpyridine platinum(II) chloride) into the active sites of these proteins (PDB codes 4GWK for 6PGD, 6E08 for G6PD, 1XAN for GR, 3CSJ for GST, and 2ZZB for TrxR) with Small-Molecule Drug Discovery Suite 2022-3 for Mac (Schrödinger, LLC). The root mean square deviation (RMSD) values between the native ligands, 3PG, NAP, HXP, CBL, and TPT conformation, and the best poses generated by this protocol were 0.20, 0.55, 0.69, 1.17, and 0.49 Å. It indicated that the Glide XP docking algorithm was qualified for docking MTX and morin to active pockets of 6PGD, G6PD, GR, GST, and TrxR enzymes, respectively.

Figures 3–7 indicate that MTX (docking scores of  $-5.30$  kcal/mol for 6PGD,  $-8.40$  kcal/mol for G6PD,  $-4.80$  kcal/mol for GR,  $-7.89$  kcal/mol for GST, and  $-4.23$  kcal/mol for TrxR) and molecular mechanics with generalized Born and surface area solvation (MM-GBSA) values of  $-4.87$  kcal/mol for 6PGD,  $-17.64$  kcal/mol for G6PD,  $-20.34$  kcal/mol for GR,  $-44.35$  kcal/mol for GST, and  $-28.17$  kcal/mol for TrxR) to morin (docking scores of  $-5.26$  kcal/mol for 6PGD,  $-7.92$  kcal/mol for G6PD,  $-4.64$  kcal/mol for GR,  $-6.41$  kcal/mol for GST, and  $-3.56$  kcal/mol for TrxR) and MM-GBSA values of  $-20.39$  kcal/mol for 6PGD,  $-34.03$  kcal/mol for G6PD,  $-17.67$  kcal/mol for GR,  $-36.04$  kcal/mol for GST, and  $-26.82$  kcal/mol for TrxR) has similar conformations, that is, H-bond, pi-pi stacking, and pi-cation interactions in these enzyme-binding pockets.

In 6PGD, MTX formed H-bond interactions at the active site with Arg288, Tyr192, and Thr263 residues. Morin interacted with Arg288 and Lys261 through H-bond (Figure 3). In G6PD, MTX made H-bonds at the active site with Lys497, Arg370, Lys403, Arg487, Glu494, Tyr507, and Tyr 503. Morin interacted with Asp421, Tyr503, Arg370, and Arg393 through H-bond, while Tyr401, Tyr507, and Trp509 residues formed hydrophobic interactions (Figure 4).

The enzyme activity after morin treatment probably increased owing to donating electrons to the substrate. In GR, MTX formed H-bond at the active site with Lys67, pi-pi stacking interactions with Tyr407 and Phe78, and hydrophobic interaction with Val74. Morin interacted with Phe78 through pi-pi stacking, Val74, Phe78, Tyr85, Phe87, and Tyr407 residues with hydrophobic interactions (Figure 5).

In GST, the hydrophobic pocket created by the side chains residues was anticipated to interact with MTX as follows: Tyr7, Phe8, Pro9, Val10, Val35, Trp38, Leu52, Pro53, Ile104, and Tyr108 residues in the active site suggest that the compound binds to the active site of GST (Figure 6).

Therefore, it was concluded that the obstruction of the active site entry may have caused this inhibitory impact; however, when morin was bound to the enzyme, an H-bond interaction formed between morin and Tyr7. In TrxR, MTX formed H-bond interaction at the Gly54, pi-pi stacking interaction with Trp114, hydrophobic interactions with Val118, Ile109, and Trp53 residues, and electrostatic interactions with Arg121. Morin interacted with Trp114 through pi-pi stacking, Ile109 and Trp53 residues through hydrophobic interactions, and Gln106 through H-bond interaction (Figure 7).

Furthermore, in an attempt to predict the dynamics and stability of enzyme-ligand complexes under physiological conditions, molecular dynamic (MD) simulations were conducted. Although frequently used docking algorithms are successful in generating active conformations of ligands, docking score algorithms are primitive. However, in our recent studies, we obtained promising binding energies in accordance with biological activities.<sup>[37–39]</sup> Thus, as a representative system, the docked poses of morin and MTX against the GST target, which yielded acceptable docking scores, were subjected to MD simulations. For each system, RMSD values of the C $\alpha$  backbone based on the reference frame backbone, the root mean square fluctuations (RMSF) for C $\alpha$ -atoms, and ligand interaction fractions were computed after 200 ns of simulation. The morin complex seems to stabilize after 100 ns, while the MTX system reaches equilibrium after just 25 ns (Figure 8).

It is worth mentioning that in both cases, the observed RMSD variations are within acceptable ranges during the whole course of the simulation. The ligand RMSD for morin-GST remains consistent throughout the simulation, whereas MTX-GST shows higher fluctuations. Nonetheless, overall variations are insignificant and lie under the permissible range of  $\sim 3$  Å. This, together with a visual inspection of the overall simulation, also confirms that both complexes have not undergone significant conformational changes and the ligands have remained stably bound to GST.

On the other hand, RMSF measures the average deviation of individual amino acid residues over time. As depicted in Figure 9, both systems yielded a steady profile having RMSF values below  $2$  Å. Notably, some amino acid residues that the ligands are interacting with (green vertical lines) have much lower RMSF values, which can be concluded as favorable contacts that help stabilize the complexes.

Ligand protein interactions were also monitored during 200 ns of simulation. The interaction fraction of the morin-GST complex shows that mainly hydrophobic interactions play critical roles. The MTX engages through hydrogen bonds emphasizing two key amino acid

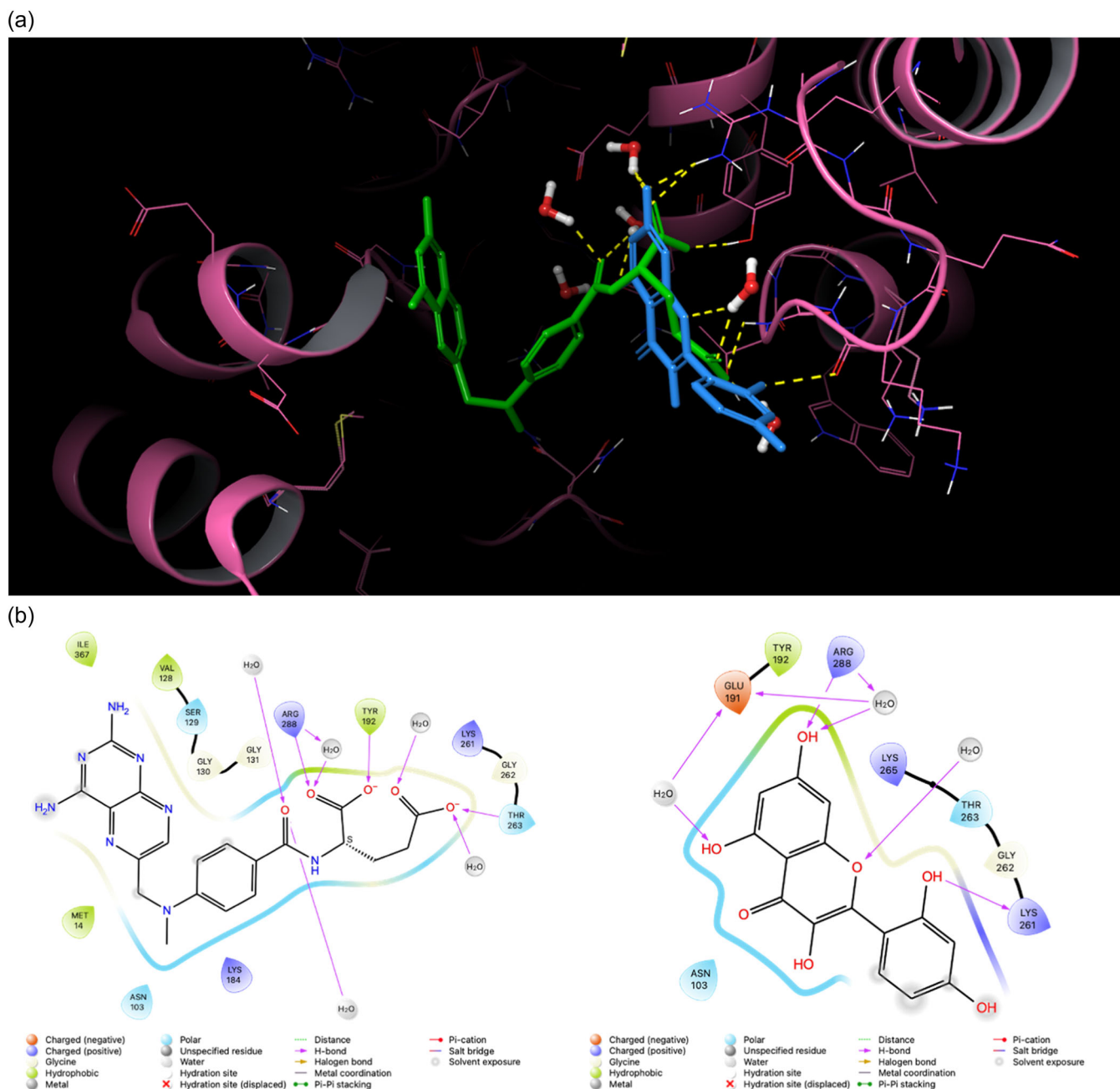


**FIGURE 3** (a) Three-dimensional (3D) interactions of methotrexate ( $C_{20}H_{22}N_8O_5$ : (4-[[2,4-diaminopteridin-6-yl)methyl](methyl)amino]benzoyl)-L-glutamic acid; green color) and morin ( $C_{15}H_{10}O_7$ : 2-(2,4-dihydroxyphenyl)-3,5,7-trihydroxy-4H-chromen-4-one; blue color) with the key amino acids within the active site of 6-phosphogluconate dehydrogenase (6PGD) (PDB code 4GWK). (b) Two-dimensional (2D) docking poses of methotrexate and morin with the key amino acids within the binding site of 6PGD (PDB code 4GWK).

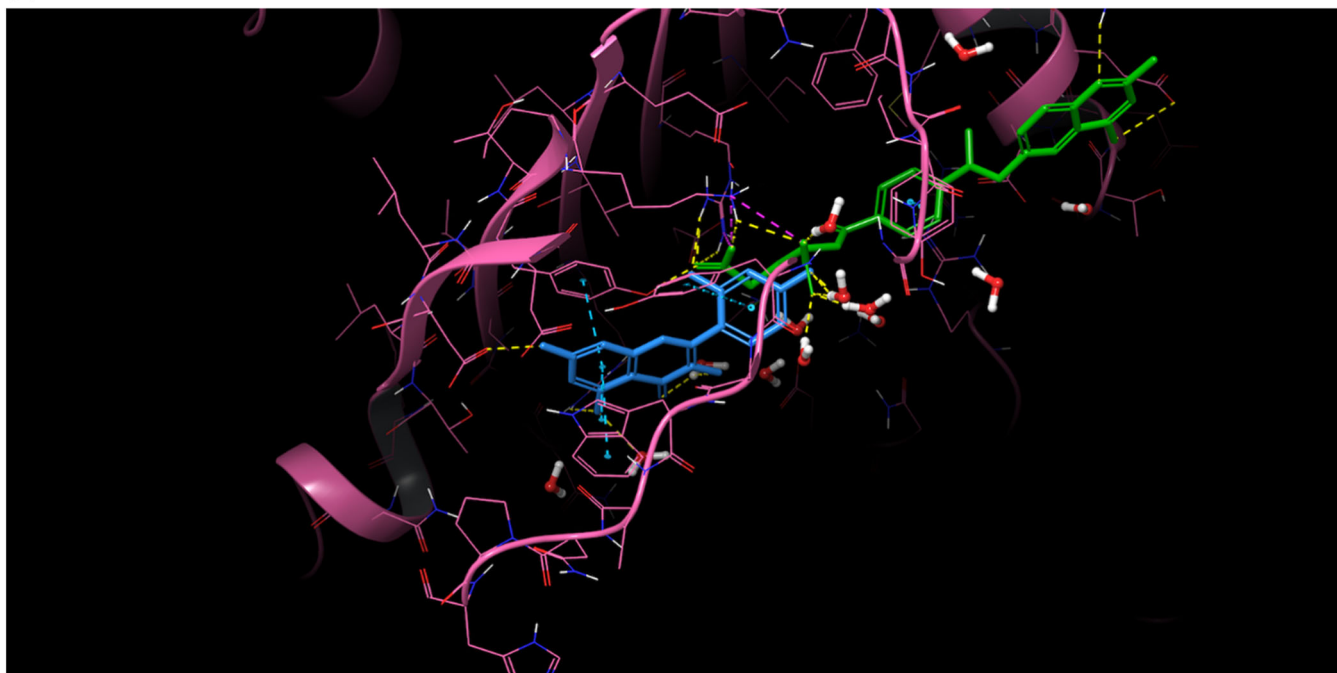
residues: Tyr7 and Arg13. The Phe8 could also help stabilize the complex via hydrophobic interactions.

### 3 | CONCLUSION

As a result, the effects of MTX and morin against various metabolic enzyme activities in rats *in vivo* and *in silico* were investigated within this study. The *in vivo* analysis results demonstrated that G6PD, 6PGD, GST, GR, and TrxR enzyme activities in the rat were

considerably decreased in the MTX-administrated group compared with the control groups while morin cotreatment significantly alleviated these effects. The docking research revealed that the dominant interactions in these enzyme-binding pockets were H-bond, pi-pi stacking, and pi-cation interactions. MD simulations confirmed the stability of morin-GST and MTX-GST against and revealed favorable ligand contacts in the binding region. The findings of this study imply that morin may be a potential treatment for MTX-induced toxicities by reducing the enzyme activity of critical regulatory enzymes.

(a)



(b)

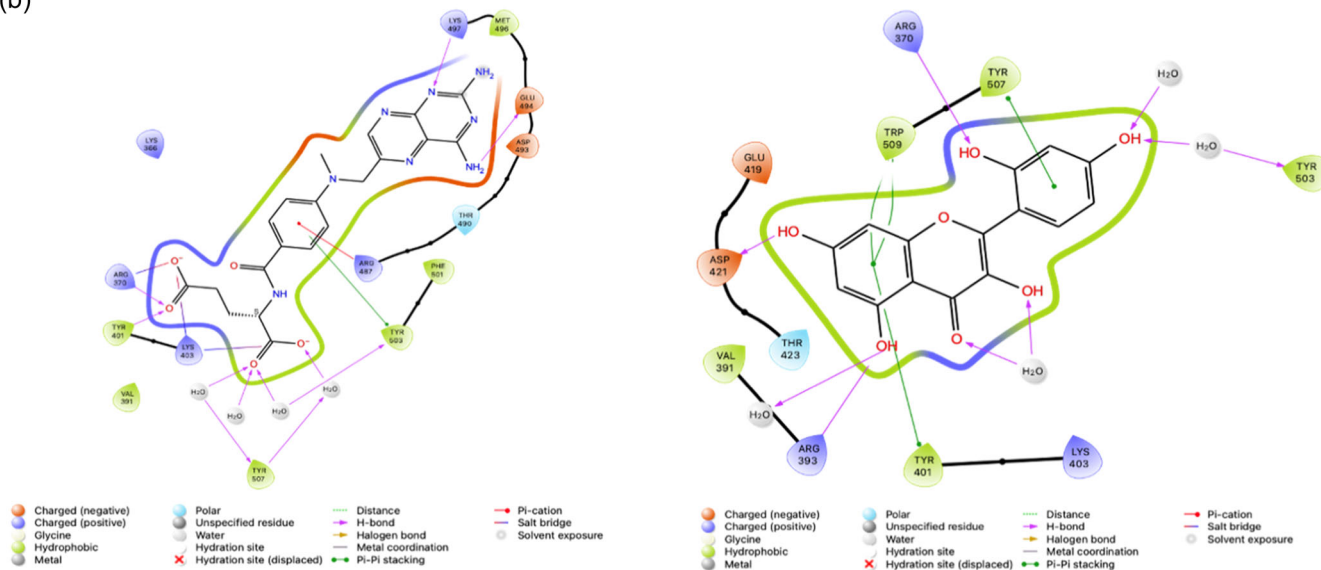


**FIGURE 4** (a) Three-dimensional (3D) interactions of methotrexate ( $C_{20}H_{22}N_8O_5$ ; 4-[[[(2,4-diaminopteridin-6-yl)methyl](methyl)amino]benzoyl]-L-glutamic acid; green color) and morin ( $C_{15}H_{10}O_7$ ; 2-(2,4-dihydroxyphenyl)-3,5,7-trihydroxy-4H-chromen-4-one; blue color) with the key amino acids within the active site of glucose-6-phosphate dehydrogenase (G6PD) (PDB code 6E08). (b) Two-dimensional (2D) docking poses of methotrexate and morin with the key amino acids within the binding site of G6PD (PDB code 6E08).

## 4 | EXPERIMENTAL

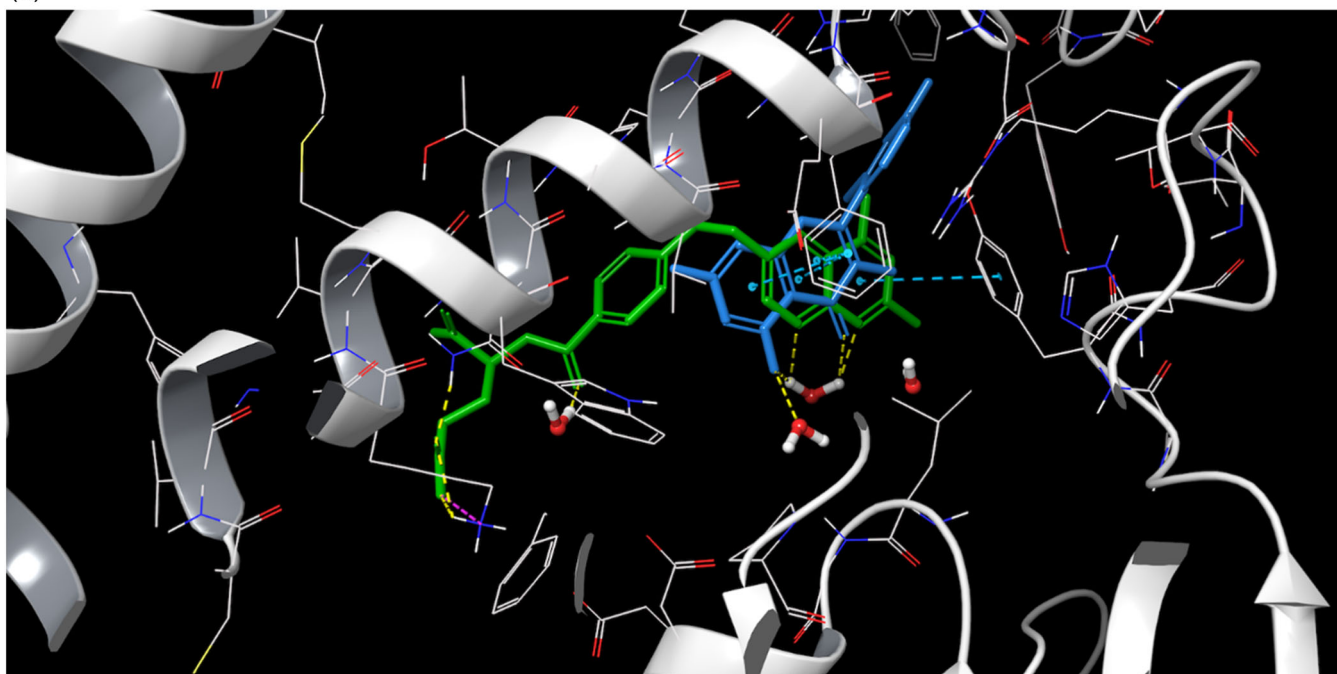
### 4.1 | Chemicals

Koçak Farma provided the injectable solution of MTX (50 mg/5 mL). All of the reagents used in the study, including morin hydrate (CAS no. 654055-01-3), were purchased from Sigma-Aldrich Co.

### 4.2 | Animals

Adult male Wistar albino rats (280–300 g) were supplied by the Experimental Research Center of Bingol University in Bingol, Turkey. Under the aforementioned facility, the animals were housed in typical laboratory settings ( $45 \pm 5\%$  humidity,  $24 \pm 1^\circ\text{C}$ , and a cycle of 12 h light: 12 h dark). The animals were given unlimited access to food and water. The Animal Experimentation Ethics Committee of

(a)



(b)

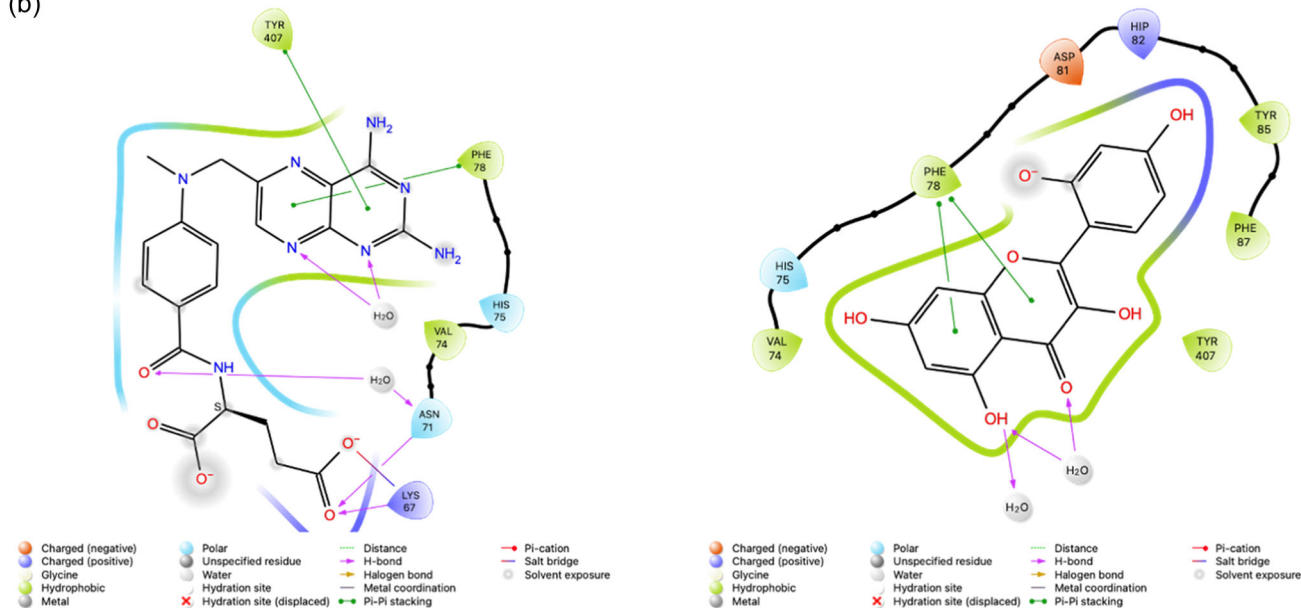


**FIGURE 5** (a) Three-dimensional (3D) interactions of methotrexate ( $C_{20}H_{22}N_8O_5$ ; 4-[[[2,4-diaminopteridin-6-yl)methyl](methyl)amino]benzoyl]-L-glutamic acid; green color) and morin ( $C_{15}H_{10}O_7$ ; 2-(2,4-dihydroxyphenyl)-3,5,7-trihydroxy-4H-chromen-4-one; blue color) with the key amino acids within the active site of glutathione reductase (GR) (PDB code 1XAN). (b) Two-dimensional (2D) docking poses of methotrexate and morin with the key amino acids within the binding site of GR (PDB code 1XAN).

Bingol University authorized all experimental protocols after they were completed in accordance with their criteria for the treatment of animals (Protocol No: 2022-E.88589).

### 4.3 | Experimental groups

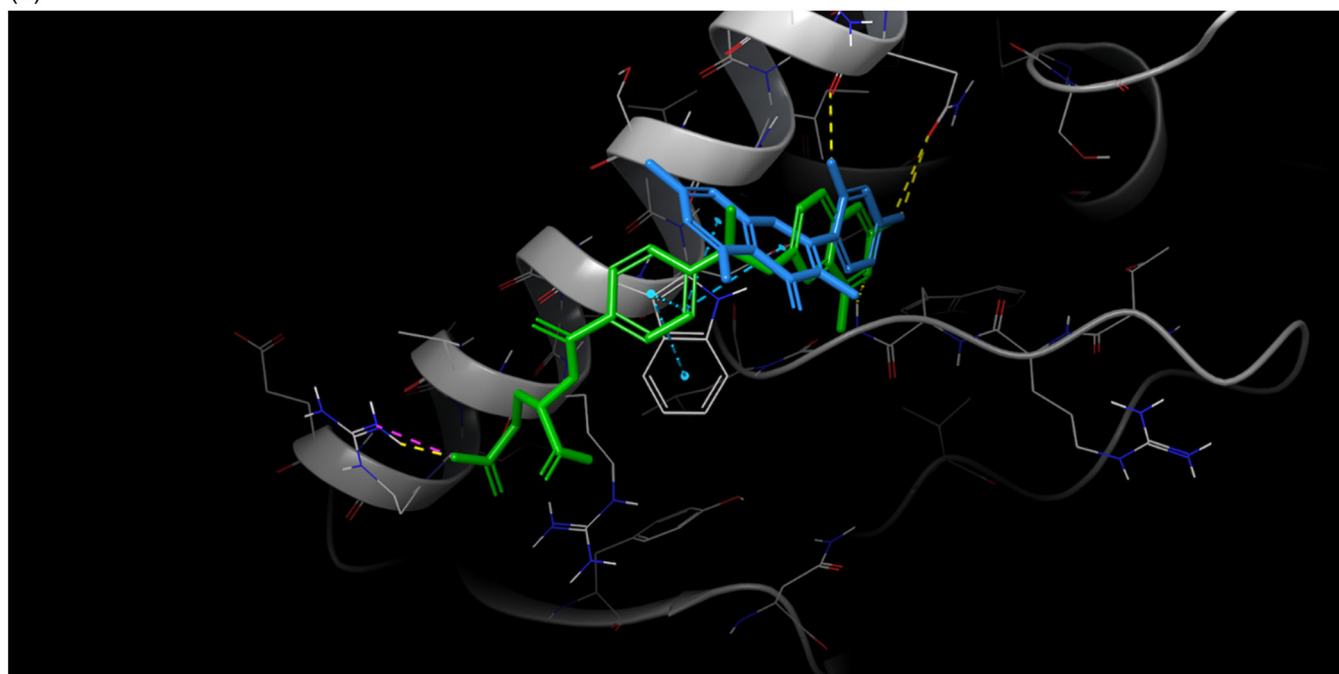
The rats were divided into five groups with seven animals in each group.

Group I (Control) received 0.9% saline via oral gavage for 10 days, and on Day 5 alone, a single saline intraperitoneal (i.p.) injection. Group II (Morin) received a single i.p. injection of saline on Day 5 only while receiving 100 mg/kg of morin orally over the course of 10 days.<sup>[40]</sup>

Group III (MTX) were given saline via oral gavage for 10 days, and on Day 5 alone, they were given a single i.p. dose of 20 mg/kg of MTX dissolved in saline.<sup>[41]</sup>



(a)



(b)

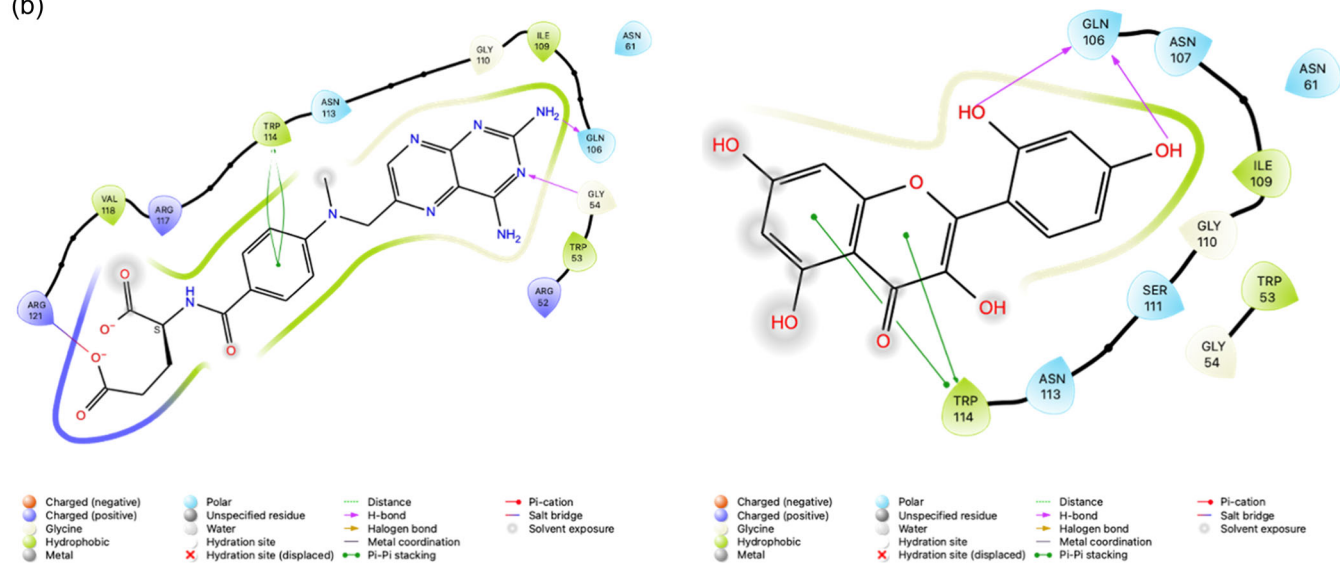


**FIGURE 7** (a) Three-dimensional (3D) interactions of methotrexate ( $C_{20}H_{22}N_8O_5$ ; (4-[[2-(2,4-diaminopteridin-6-yl)methyl](methyl)amino]benzoyl)-L-glutamic acid; green color) and morin ( $C_{15}H_{10}O_7$ ; 2-(2,4-dihydroxyphenyl)-3,5,7-trihydroxy-4H-chromen-4-one; blue color) with the key amino acids within the active site of thioredoxin reductase (TrxR) (PDB code 2ZZB). (b) Two-dimensional (2D) docking poses of methotrexate and morin with the key amino acids within the binding site of TrxR (PDB code 2ZZB).

insoluble components. When the hemolysate was separated, the supernatant was collected for use in the analyses.

#### 4.5 | Determination of the enzyme activities (G6PD, 6PGD, GR, GST and TrxR enzymes)

The investigation involved spectrophotometric measurements of G6PD, 6PGD, GR, GST, and TrxR enzyme activities at predetermined wavelengths. The enzyme activities of G6PD and 6PGD were

measured as stated in our previous study.<sup>[43]</sup> The solution used to measure the activities of G6PD and 6PGD included 0.6 mM G6P/6PGA, 0.2 mM NADP<sup>+</sup>, 0.5 mM EDTA, and 0.01 mM MgCl<sub>2</sub> at a pH of 8.0. GR enzyme activity was measured spectrophotometrically at 340 nm.<sup>[44]</sup> The mixture used to test for GR contains 2 mM NADPH, 20 mM GSSG, and 0.1 mM K-phosphate. TrxR enzyme activity was assessed using the Luthman and Holmgren<sup>[45]</sup> method, and measurements were made at a wavelength of 412 nm. GST was assayed using a combination that included 100 mM K-phosphate, 10 mM EDTA, 0.2 mM NADPH, 0.2 mg/mL bovine serum albumin (BSA), and 5 mM

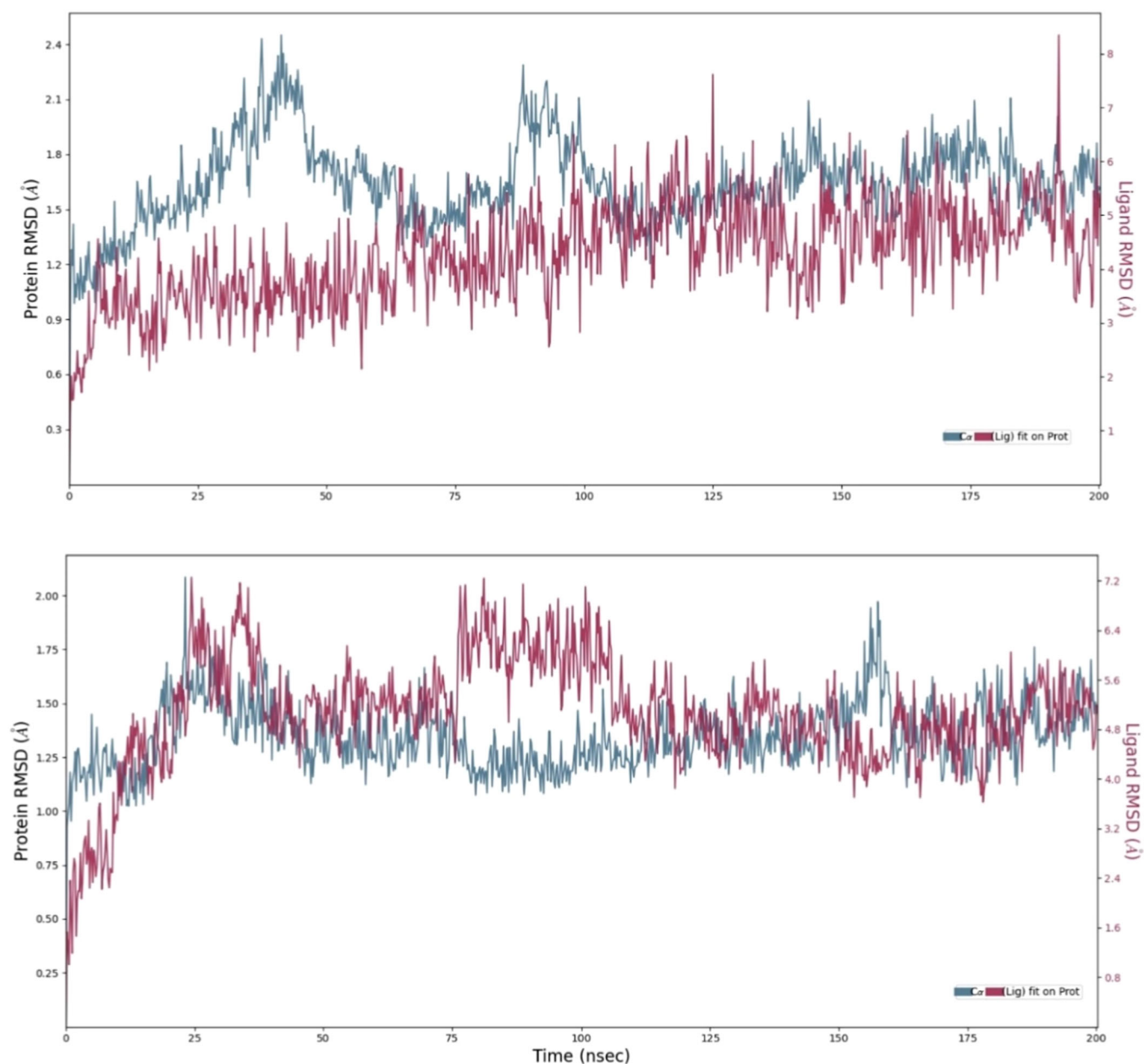


**FIGURE 8** Protein (marin) and ligand (red) root mean square deviation (RMSD) plot for morin (C<sub>15</sub>H<sub>10</sub>O<sub>7</sub>: 2-(2,4-dihydroxyphenyl)-3,5,7-trihydroxy-4H-chromen-4-one)-GST (top) and methotrexate (C<sub>20</sub>H<sub>22</sub>N<sub>8</sub>O<sub>5</sub>: (4-(((2,4-diaminopteridin-6-yl)methyl)(methyl)amino)benzoyl)-L-glutamic acid)-glutathione-S-transferase (GST) systems.

5,5'-dithiobis 2-nitrobenzoic acid (DTNB). In the assay medium, 20 mM GSH, 25 mM CDNB, 0.1 mM EDTA, and 0.1 mM K-phosphate were used.<sup>[46]</sup> Enzyme activities were expressed as EU/mg protein. An enzyme unit was defined as the quantity of enzyme needed to catalyze the reaction of 1 μmol of substrate per minute at 25°C.

#### 4.6 | The determination of protein quantity

The Bradford technique was used to determine the protein quantity. The reference protein for this analysis was BSA.<sup>[47]</sup>

#### 4.7 | In silico study

As previously reported,<sup>[48-50]</sup> in silico calculations were carried out using the Small-Molecule Drug Discovery Suite 2022-3 for Mac (Schrödinger, LLC). Protein Data Bank (<http://www.rcsb.org/>) was utilized to obtain the crystal structures of 6PGD (PDB code 4GWK; resolution: 1.53 Å, A chain),<sup>[51]</sup> G6PD (PDB code 6E08; resolution: 1.90 Å, A chain),<sup>[52]</sup> GR (PDB code 1XAN; resolution: 2.00 Å, A chain),<sup>[53]</sup> GST (PDB code 3CSJ; resolution: 1.90 Å, B chain),<sup>[54]</sup> and TrxR (PDB code 2ZZB; resolution: 3.20 Å, B chain).<sup>[55]</sup> The structural optimization of 4GWK, 6E08, 1XAN, 3CSJ, and 2ZZB was performed using the

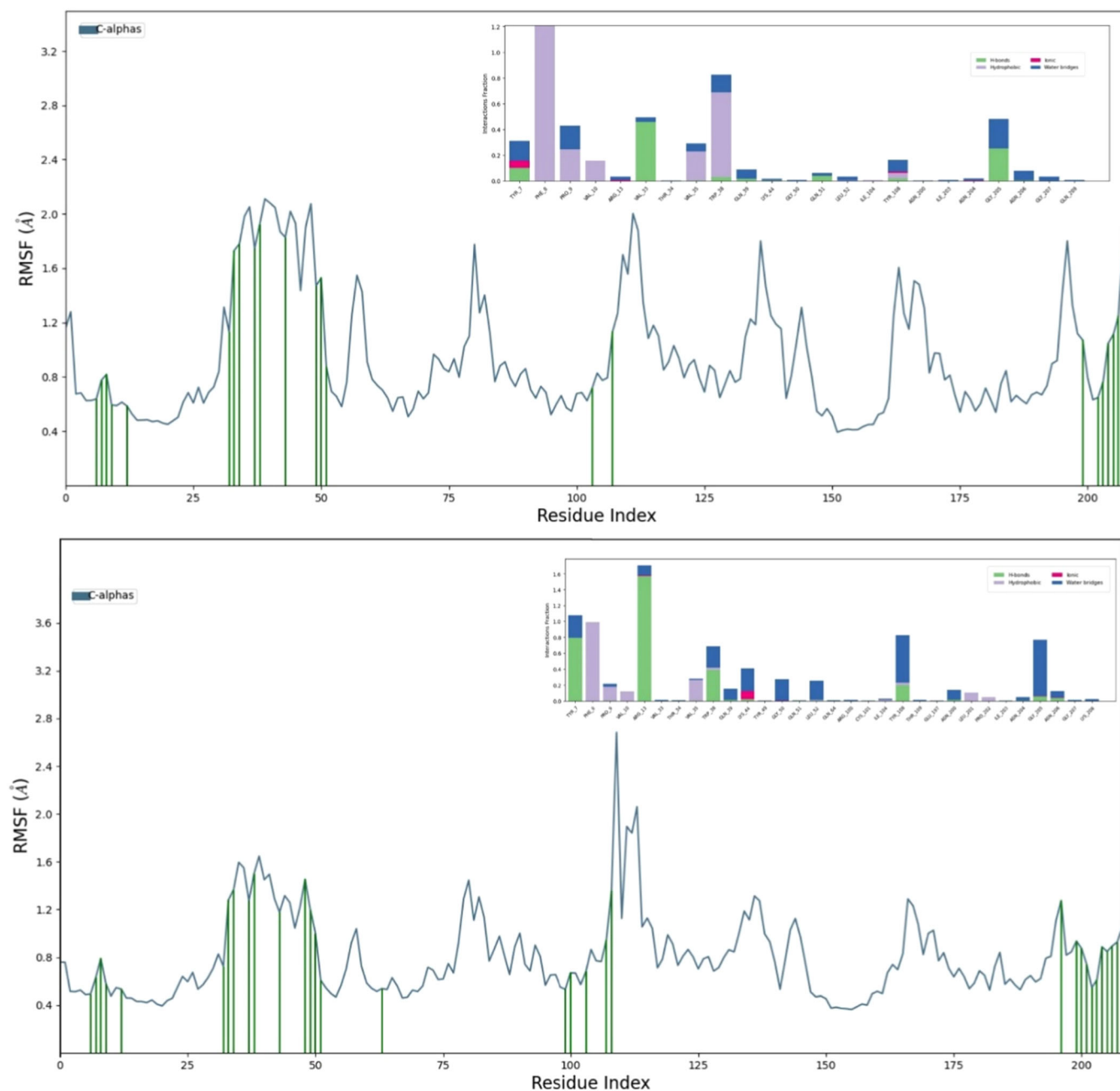


**FIGURE 9** Root mean square fluctuations (RMSF) plots for morin ( $C_{15}H_{10}O_7$ : 2-(2,4-dihydroxyphenyl)-3,5,7-trihydroxy-4H-chromen-4-one)-GST (top) and methotrexate ( $C_{20}H_{22}N_8O_5$ : (4-[[[2,4-diaminopteridin-6-yl)methyl](methyl)amino]benzoyl)-L-glutamic acid)-glutathione-S-transferase (GST) systems. Figure insets show ligand interaction diagrams during 200 ns molecular dynamic (MD) simulations.

Protein Preparation Wizard program<sup>[56]</sup> in the Maestro panel.<sup>[57]</sup> The SiteMap algorithm<sup>[58]</sup> was used to predict the active sites of proteins.<sup>[59–61]</sup> The most likely ionization states in the OPLS4 force field<sup>[62]</sup> at  $pH\ 7.4 \pm 0.5$  were generated using Epik<sup>[63]</sup> and the LigPrep program.<sup>[64]</sup> Energy grids were built using the Receptor Grid Generation application with its default settings.<sup>[65,66]</sup> Calculations for the glide extra precision (XP)<sup>[67,68]</sup> were done with the help of the docking score tool. Additionally, utilizing the protein–ligand complexes 4GWK, 6E08, 1XAN, 3CSJ, and 2ZZB, the MM-GBSA's to forecast relative binding affinity in the variable-dielectric surfacegeneralized born energy

model<sup>[69]</sup> and OPLS4 force field has been assessed. Furthermore, the Desmond module was used for MD simulations.<sup>[70]</sup> An orthorhombic simulation box with the reparameterized transferable intermolecularpotential with a 4-point water model was prepared using the system builder panel. Subsequent to neutralizing the system with sodium ions, physiological conditions were mimicked by adding 0.15 M NaCl concentration. Salt and ion placement were excluded within 20 Å of the ligand. The system was first relaxed by default, and then MD was performed for 200 ns in an NPT ensemble with a recording interval of 200 ps, which finally yielded approximately 1000 frames.

## 4.8 | Statistical analysis

For the statistical analysis, SPSS Statistics 20 was employed. The data were presented as mean SD. To compare the differences between the groups, one-way analysis of variance (ANOVA) and Tukey's post hoc least significant difference (LSD) were utilized. When the  $p$ -value was 0.05, the difference between the groups was deemed significant.

## ACKNOWLEDGMENTS

The authors thank Assoc. Prof. Ekrem Darendelioglu for contributions to this study.

## CONFLICTS OF INTEREST STATEMENT

The authors declare no conflicts of interest.

## ORCID

Cuneyt Caglayan  <http://orcid.org/0000-0001-5608-554X>

Abdullah Ece  <http://orcid.org/0000-0002-3087-5145>

Şükrü Beydemir  <http://orcid.org/0000-0003-3667-6902>

## REFERENCES

- Y. Bedoui, X. Guillot, J. Sélambarom, P. Guiraud, C. Giry, M. C. Jaffar-Bandjee, S. Ralandison, P. Gasque, in *Int. J. Mol. Sci.* **2019**, *20*, 5023. <https://doi.org/10.3390/ijms20205023>
- B. N. Cronstein, T. M. Aune, *Nat. Rev. Rheumatol.* **2020**, *16*, 145. <https://doi.org/10.1038/s41584-020-0373-9>
- B. Friedman, B. Cronstein, *Joint Bone Spine* **2019**, *86*, 301. <https://doi.org/10.1016/j.jbspin.2018.07.004>
- S. A. Rajput, X.-Q. Wang, H.-C. Yan, *Biomed. Pharmacother.* **2021**, *138*, 111511. <https://doi.org/10.1016/j.biopha.2021.111511>
- C. Gur, F. M. Kandemir, E. Darendelioglu, C. Caglayan, S. Kucukler, O. Kandemir, M. Ileriturk, *Environ. Sci. Pollut. Res.* **2021**, *28*, 49808. <https://doi.org/10.1007/s11356-021-14049-4>
- S. Solairaja, M. Q. Andrabi, N. R. Dunna, S. Venkatabalasubramanian, *Nutr. Cancer* **2021**, *73*, 927. <https://doi.org/10.1080/01635581.2020.1778747>
- F. M. Kandemir, S. Yıldırım, S. Kucukler, C. Caglayan, E. Darendelioglu, M. B. Dortbudak, *Food Chem. Toxicol.* **2020**, *138*, 111190. <https://doi.org/10.1016/j.fct.2020.111190>
- H. Çelik, S. Kucukler, S. Çomaklı, S. Özdemir, C. Caglayan, A. Yardım, F. M. Kandemir, *Neurotoxicology* **2020**, *76*, 126. <https://doi.org/10.1016/j.neuro.2019.11.004>
- S. Mottaghi, H. Abbaszadeh, *Phytother. Res.* **2021**, *35*, 6843. <https://doi.org/10.1002/ptr.7270>
- E. S. L. Chan, B. N. Cronstein, *Nat. Rev. Rheumatol.* **2010**, *6*, 175. <https://doi.org/10.1038/nrrheum.2010.5>
- V. Maksimovic, Z. Pavlovic-Popovic, S. Vukmirovic, J. Cvejic, A. Mooranian, H. Al-Salami, M. Mikov, S. Golocorbin-Kon, *Mol. Biol. Rep.* **2020**, *47*, 4699. <https://doi.org/10.1007/s11033-020-05481-9>
- E. Ozturk, D. Karabulut, A. T. Akin, E. Kaymak, N. Kuloglu, B. Yakan, *J. Mol. Histol.* **2022**, *53*, 133. <https://doi.org/10.1007/s10735-021-10027-9>
- H. E. Kızıl, C. Caglayan, E. Darendelioglu, A. Ayna, C. Gür, F. M. Kandemir, S. Küçükler, *Mol. Biol. Rep.* **2023**, *50*, 3479. <https://doi.org/10.1007/s11033-023-08286-8>
- F. M. Kandemir, S. Kucukler, C. Caglayan, C. Gur, A. A. Batil, İ. Gülçin, *J. Food Biochem.* **2017**, *41*, e12398. <https://doi.org/10.1111/jfbc.12398>
- B. Varişlı, C. Caglayan, F. M. Kandemir, C. Gür, İ. Bayav, A. Genç, *Mol. Biol. Rep.* **2022**, *49*, 9641. <https://doi.org/10.1007/s11033-022-07873-5>
- R. Aslankoc, O. Ozmen, A. Yalcın, *Biotech. Histochem.* **2022**, *97*, 382. <https://doi.org/10.1080/10520295.2021.2004616>
- R. R. Singh, K. M. Reindl, in *Antioxidants* **2021**, *10*, 701. <https://doi.org/10.3390/antiox10050701>
- F. Türkan, Z. Huyut, P. Taslimi, M. T. Huyut, İ. Gülçin, *Drug Chem. Toxicol.* **2020**, *43*, 423. <https://doi.org/10.1080/01480545.2018.1497644>
- F. Türkan, P. Taslimi, S. M. Abdalrazaq, A. Aras, Y. Erden, H. U. Celebioglu, B. Tuzun, M. S. Ağırtaş, İ. Gülçin, *J. Biomol. Struct. Dyn.* **2021**, *39*, 3693. <https://doi.org/10.1080/07391102.2020.1763200>
- A. Ayna, L. Khosnaw, Y. Temel, M. Ciftci, *Curr. Drug Metab.* **2021**, *22*, 308. <https://doi.org/10.2174/1389200222666210118102700>
- J. Song, H. Sun, S. Zhang, C. Shan, *Life* **2022**, *12*, 271. <https://doi.org/10.3390/life12020271>
- L. Luzzatto, M. Ally, R. Notaro, *Blood* **2020**, *136*, 1225. <https://doi.org/10.1182/blood.2019000944>
- Y. Temel, A. Ayna, İ. Hamdi Shafeeq, M. Ciftci, *Drug Chem. Toxicol.* **2020**, *43*, 219. <https://doi.org/10.1080/01480545.2018.1481083>
- S. Adem, M. Ciftci, *J. Biochem. Mol. Toxicol.* **2016**, *30*, 295. <https://doi.org/10.1002/jbt.21793>
- G. Kizilbay, M. Karaman, *J. Biomol. Struct. Dyn.* **2022**, *40*, 204. <https://doi.org/10.1080/07391102.2020.1811155>
- E. Akkemik, H. Budak, M. Ciftci, *J. Enzyme Inhib. Med. Chem.* **2010**, *25*, 871. <https://doi.org/10.3109/14756360903489581>
- B. Çalışkan, A. Öztürk Kesebir, Y. Demir, İ. Akyol Salman, *Biotechnol. Appl. Biochem.* **2022**, *69*. <https://doi.org/10.1002/bab.2107>
- K. Işık, E. Soydan, *J. Enzyme Inhib. Med. Chem.* **2023**, *38*, 2167078. <https://doi.org/10.1080/14756366.2023.2167078>
- D. A. Averill-Bates, *Vitam. Horm.* **2023**, *121*, 109. <https://doi.org/10.1016/bs.vh.2022.09.002>
- Y. Demir, C. Türkeş, Ö. İ. Küfrevioğlu, Ş. Beydemir, *Chem. Biodivers.* **2023**, *20*, 202200656. <https://doi.org/10.1002/cbdv.202200656>
- X. Li, M. Ni, X. Xu, W. Chen, *J. Enzyme Inhib. Med. Chem.* **2020**, *35*, 1773. <https://doi.org/10.1080/14756366.2020.1822828>
- E. Kocaoğlu, O. Talaz, H. Çavdar, M. Şentürk, C. T. Supuran, D. Ekinci, *J. Enzyme Inhib. Med. Chem.* **2019**, *34*, 51. <https://doi.org/10.1080/14756366.2018.1520228>
- P. Güller, M. Karaman, U. Güller, M. Aksoy, Ö. İ. Küfrevioğlu, *J. Biomol. Struct. Dyn.* **2021**, *39*, 1744. <https://doi.org/10.1080/07391102.2020.1738962>
- S. Tiwari, M. Wadhawan, N. Singh, S. Rathaur, *J. Proteomics* **2015**, *113*, 435. <https://doi.org/10.1016/j.jprot.2014.10.007>
- F. Y. Shao, Z. Y. Du, D. L. Ma, W. B. Chen, W. Y. Fu, B. B. Ruan, W. Rui, J. X. Zhang, S. Wang, N. S. Wong, H. Xiao, M. M. Li, X. Liu, Q. Y. Liu, X. D. Zhou, H. Z. Yan, Y. F. Wang, C. Y. Chen, Z. Liu, H. Y. Chen, *Oncotarget* **2015**, *6*, 30939. <https://doi.org/10.18632/oncotarget.5132>
- F. Saccoccia, F. Angelucci, G. Boumis, D. Carotti, G. Desiato, A. E. Miele, A. Bellelli, *Curr. Protein Pept. Sci.* **2014**, *15*, 621.
- M. Er, B. Ergüven, H. Tahtacı, A. Onaran, T. Karakurt, A. Ece, *Med. Chem. Res.* **2017**, *26*, 615. <https://doi.org/10.1007/s00044-017-1782-4>
- F. Başoğlu, N. Ulusoy-Güzeldemirci, G. Akalın-Çiftçi, S. Çetinkaya, A. Ece, *Chem. Biol. Drug Des.* **2021**, *98*, 270. <https://doi.org/10.1111/cbdd.13896>
- H. Tahtacı, H. Karacık, A. Ece, M. Er, M. G. Şeker, *Mol. Inf.* **2018**, *37*, 1700083. <https://doi.org/10.1002/minf.201700083>
- M. Kuzu, S. Yıldırım, F. M. Kandemir, S. Küçükler, C. Çağlayan, E. Türk, M. B. Dörtbudak, *Chem.-Biol. Interact.* **2019**, *308*, 89. <https://doi.org/10.1016/j.cbi.2019.05.017>

- [41] E. Hassanein, A. S. Shalkami, M. M. Khalaf, W. R. Mohamed, R. Hemeida, *Biomed. Pharmacother.* **2019**, *109*, 47. <https://doi.org/10.1016/j.biopha.2018.10.088>
- [42] Y. Temel, C. Çağlayan, B. M. Ahmed, F. M. Kandemir, M. Çiftci, *Naunyn-Schmiedeberg's Arch. Pharmacol.* **2021**, *394*, 645. <https://doi.org/10.1007/s00210-020-01987-y>
- [43] S. Bayindir, A. Ayna, Y. Temel, M. Çiftci, *Turk. J. Chem.* **2018**, *42*, 332. <https://doi.org/10.3906/kim-1706-51>
- [44] M. R. Kıvanç, V. Türkoglu, *Biomed. Chromatogr.* **2019**, *33*, e4560. <https://doi.org/10.1002/bmc.4560>
- [45] M. Luthman, A. Holmgren, *Biochemistry* **1982**, *21*, 6628. <https://doi.org/10.1021/bi00269a003>
- [46] Y. Temel, M. Ş. Taysi, *Biol. Trace Elem. Res.* **2019**, *191*, 177. <https://doi.org/10.1007/s12011-018-1601-x>
- [47] M. M. Bradford, *Anal. Biochem.* **1976**, *72*, 248. [https://doi.org/10.1016/0003-2697\(76\)90527-3](https://doi.org/10.1016/0003-2697(76)90527-3)
- [48] G. Yapar, H. Esra Duran, N. Lolak, S. Akocak, C. Türkeş, M. Durgun, M. Işık, Ş. Beydemir, *Bioorg. Chem.* **2021**, *117*, 105473. <https://doi.org/10.1016/j.bioorg.2021.105473>
- [49] A. Buza, C. Türkeş, M. Arslan, Y. Demir, B. Dincer, A. R. Nixha, Ş. Beydemir, *Int. J. Biol. Macromol.* **2023**, *239*, 124232. <https://doi.org/10.1016/j.ijbiomac.2023.124232>
- [50] C. Kakakhan, C. Türkeş, Ö. Güleç, Y. Demir, M. Arslan, G. Özkemahlı, Ş. Beydemir, *Bioorg. Med. Chem.* **2023**, *77*, 117111. <https://doi.org/10.1016/j.bmc.2022.117111>
- [51] T. Hitosugi, L. Zhou, S. Elf, J. Fan, H.-B. Kang, J. H. Seo, C. Shan, Q. Dai, L. Zhang, J. Xie, T.-L. Gu, P. Jin, M. Alečković, G. LeRoy, Y. Kang, J. A. Sudderth, R. J. DeBerardinis, C.-H. Luan, G. Z. Chen, S. Muller, D. M. Shin, T. K. Owonikoko, S. Lonial, M. L. Arellano, H. J. Khoury, F. R. Khuri, B. H. Lee, K. Ye, T. J. Boggon, S. Kang, C. He, J. Chen, *Cancer Cell* **2012**, *22*, 585. <https://doi.org/10.1016/j.ccr.2012.09.020>
- [52] S. Hwang, K. Mruk, S. Rahighi, A. G. Raub, C.-H. Chen, L. E. Dorn, N. Horikoshi, S. Wakatsuki, J. K. Chen, D. Mochly-Rosen, *Nat. Commun.* **2018**, *9*, 4045. <https://doi.org/10.1038/s41467-018-06447-z>
- [53] S. N. Savvides, P. A. Karplus, *J. Biol. Chem.* **1996**, *271*, 8101. <https://doi.org/10.1074/jbc.271.14.8101>
- [54] L. J. Parker, S. Ciccone, L. C. Italiano, A. Primavera, A. J. Oakley, C. J. Morton, N. C. Hancock, M. L. Bello, M. W. Parker, *J. Mol. Biol.* **2008**, *380*, 131. <https://doi.org/10.1016/j.jmb.2008.04.066>
- [55] Y.-C. Lo, T.-P. Ko, W.-C. Su, T.-L. Su, A. H.-J. Wang, *J. Inorg. Biochem.* **2009**, *103*, 1082. <https://doi.org/10.1016/j.jinorgbio.2009.05.006>
- [56] G. Madhavi Sastry, M. Adzhigirey, T. Day, R. Annabhimoju, W. Sherman, *J. Comput.-Aided Mol. Des.* **2013**, *27*, 221. <https://doi.org/10.1007/s10822-013-9644-8>
- [57] D. Osmaniye, C. Türkeş, Y. Demir, Y. Özkay, Ş. Beydemir, Z. A. Kaplancıklı, *Arch. Pharm.* **2022**, *355*, 2200132. <https://doi.org/10.1002/ardp.202200132>
- [58] T. A. Halgren, *J. Chem. Inf. Model.* **2009**, *49*, 377. <https://doi.org/10.1021/ci800324m>
- [59] K. Yazarlı, E. B. Ozer, S. Bayindir, C. Çağlayan, C. Türkeş, S. Beydemir, *J. Mol. Struct.* **2023**, *1276*, 134783. <https://doi.org/10.1016/j.molstruc.2022.134783>
- [60] Ö. Güleç, C. Türkeş, M. Arslan, Y. Demir, Y. Yeni, A. Hacımüftüoğlu, E. Ereminsoy, Ö. İ. Küfrevioğlu, Ş. Beydemir, *Mol. Divers.* **2022**, *26*, 2825. <https://doi.org/10.1007/s11030-022-10422-8>
- [61] C. Türkeş, Y. Demir, Ş. Beydemir, *ChemistrySelect* **2021**, *6*, 11915. <https://doi.org/10.1002/slct.202103197>
- [62] C. Türkeş, Y. Demir, A. Biçer, G. T. Cin, M. S. Gültekin, Ş. Beydemir, *ChemistrySelect* **2023**, *8*, e202204350. <https://doi.org/10.1002/slct.202204350>
- [63] J. C. Shelley, A. Cholleti, L. L. Frye, J. R. Greenwood, M. R. Timlin, M. Uchimaya, *J. Comput.-Aided Mol. Des.* **2007**, *21*, 681. <https://doi.org/10.1007/s10822-007-9133-z>
- [64] G. M. Sastry, V. S. S. Inakollu, W. Sherman, *J. Chem. Inf. Model.* **2013**, *53*, 1531. <https://doi.org/10.1021/ci300463g>
- [65] C. Türkeş, A. Ö. Kesebir, Y. Demir, Ö. İ. Küfrevioğlu, Ş. Beydemir, *ChemistrySelect* **2021**, *6*, 11137.
- [66] C. Türkeş, *J. Mol. Recognit.* **2023**, *12*, 3063. <https://doi.org/10.1002/jmr.3063>
- [67] R. A. Friesner, J. L. Banks, R. B. Murphy, T. A. Halgren, J. J. Klicic, D. T. Mainz, M. P. Repasky, E. H. Knoll, M. Shelley, J. K. Perry, D. E. Shaw, P. Francis, P. S. Shenkin, *J. Med. Chem.* **2004**, *47*, 1739. <https://doi.org/10.1021/jm0306430>
- [68] T. A. Halgren, R. B. Murphy, R. A. Friesner, H. S. Beard, L. L. Frye, W. T. Pollard, J. L. Banks, *J. Med. Chem.* **2004**, *47*, 1750. <https://doi.org/10.1021/jm030644s>
- [69] G. Barreiro, C. R. W. Guimarães, I. Tubert-Brohman, T. M. Lyons, J. Tirado-Rives, W. L. Jorgensen, *J. Chem. Inf. Model.* **2007**, *47*, 2416. <https://doi.org/10.1021/ci700271z>
- [70] Ö. Güleç, C. Türkeş, M. Arslan, Y. Demir, B. Dincer, A. Ece, Ş. Beydemir, *J. Biomol. Struct. Dyn.* **2023**, *42*, 1. <https://doi.org/10.1080/07391102.2023.2240889>

**How to cite this article:** C. Çağlayan, Y. Temel, C. Türkeş, A. Ayna, A. Ece, Ş. Beydemir, *Arch. Pharm.* **2024**;357:e2300497. <https://doi.org/10.1002/ardp.202300497>